New Phytologist

# Where do roots take up water? Neutron radiography of water flow into the roots of transpiring plants growing in soil

**Mohsen Zarebanadkouki, Yangmin X. Kim and Andrea Carminati**

Soil Hydrology, Georg August University of Göttingen, 37077 Göttingen, Germany

Author for correspondence:
*Mohsen Zarebanadkouki*
*Tel: +49 (0) 551 3913517*
*Email: mzareba@gwdg.de*

Received: *25 February 2013*
Accepted: *11 April 2013*

*New Phytologist* (2013) **199:** 1034–1044
**doi**: 10.1111/nph.12330

**Key words:** axial water flux, deuterated water ($D_2O$), diffusional permeability, *Lupinus albus* (lupin), neutron radiography, radial water flux, root water uptake.

## Summary

• Where and how fast does water flow from soil into roots? The answer to this question requires direct and *in situ* measurement of local flow of water into roots of transpiring plants growing in soil.

• We used neutron radiography to trace the transport of deuterated water ($D_2O$) in lupin (*Lupinus albus*) roots. Lupins were grown in aluminum containers (30 × 25 × 1 cm) filled with sandy soil. $D_2O$ was injected in different soil regions and its transport in soil and roots was monitored by neutron radiography. The transport of water into roots was then quantified using a convection–diffusion model of $D_2O$ transport into roots.

• The results showed that water uptake was not uniform along roots. Water uptake was higher in the upper soil layers than in the lower ones. Along an individual root, the radial flux was higher in the proximal segments than in the distal segments.

• In lupins, most of the water uptake occurred in lateral roots. The function of the taproot was to collect water from laterals and transport it to the shoot. This function is ensured by a low radial conductivity and a high axial conductivity. Lupin root architecture seems well designed to take up water from deep soil layers.

## Introduction

Where and how fast do roots take up water? Despite its importance in plant and soil sciences, there is limited experimental information on the location of water uptake along roots of transpiring plants growing in soil. Root water uptake is a dynamic process that involves complex interactions among atmosphere, plants and soil. The location of water flow into roots depends on the relative importance of the hydraulic conductivities of the root–soil interface, the radial path across roots, and the axial path along the xylem (Landsberg & Fowkes, 1978; Steudle & Peterson, 1998; Draye *et al.*, 2010).

Owing to the porous nature of the roots, the relative importance of radial and axial conductances determines the profile of water uptake along roots (Landsberg & Fowkes, 1978; Frensch *et al.*, 1996; Hsiao & Xu, 1995; Zwieniecki *et al.*, 2003). During transpiration, the initiating low water potential at the proximal end of a root dissipates along the root and a lower tension transmits to the distal parts. A combination of high radial conductivity and low axial conductivity results in a big pressure dissipation along the xylem and a reduced uptake from the distal parts. Conversely, low radial conductivity and high axial conductivity result in uniform water uptake along the root.

Root hydraulic conductivities vary along the root system during root maturation as well as in response to external conditions. As roots mature, their radial hydraulic conductivities decrease as a consequence of anatomical modification of the root tissue (Steudle & Peterson, 1998; Enstone *et al.*, 2003; Bramley *et al.*, 2009; Knipfer & Fricke, 2010). Decrease of the radial hydraulic conductivity with age shifts the water uptake zone to the distal root segments. The axial conductivity varies along root length as a consequence of the differentiation of early metaxylem vessels during the developmental stage of plants and the formation of secondary xylem during secondary growth (Varney & Canny, 1993; McCully, 1995; Vercambre *et al.*, 2002; Bramley *et al.*, 2009). An increase of axial hydraulic conductivity through root maturation helps to redistribute the water uptake zone more evenly along the roots. As the soil dries, the soil hydraulic conductivity may further limit root water uptake. As the soil typically dries more quickly in the upper layers (as a result of evaporation, gravity and higher root length density), the water uptake zone is expected to move downwards along the soil profile.

To date, it has been difficult to measure directly where roots take up water in soil. Thanks to recent advances in imaging methods, it is now possible to monitor the spatiotemporal distribution of roots and water content in soil (Pierret *et al.*, 2003; Garrigues *et al.*, 2006; Pohlmeier *et al.*, 2008; Moradi *et al.*, 2011). In these studies, root water uptake was indirectly estimated from the decrease in soil water content near the roots. However, simulations of water flow in soil demonstrated that water uptake is not equal to the change in water content, because of soil water redistribution. Therefore, observations of water content change must be coupled with models of water flow in roots and soil (Javaux *et al.*, 2008). Such methods require accurate knowledge of root and soil hydraulic properties and cannot differentiate between uptake rates of neighboring roots.

In this study, we tested a new method to measure the local fluxes of water into and along the root system of transpiring plants growing in soil. The method consists of monitoring the transport of deuterated water ($D_2O$) into roots by means of time-series neutron radiography. Neutron radiography is an imaging technique that has a high sensitivity to normal water ($H_2O$). Compared with normal water, $D_2O$ is almost transparent in neutron radiography and its transport into roots can be monitored at high temporal and spatial resolution. The method was introduced by Zarebanadkouki *et al.*(2012), who applied it to the lateral roots of lupins at a specific location of the root system. The objective of the present study was to apply the technique to different locations along the roots of lupins. The model introduced by Zarebanadkouki *et al.*(2012) has been extended to the case of roots partly immersed in $H_2O$ and partly in $D_2O$. Additionally, the description of the radial pathway of water into roots has been generalized to allow a varying importance of apoplastic and cell-to-cell flow. The questions we addressed are as follows: where does water enter the roots of lupins; and is the water uptake higher in the taproot or in the laterals, and in the proximal or in the distal segments? In these experiments, the soil was kept wet. In further studies, we will investigate how the uptake patterns change as the soil dries.

## Materials and Methods

### Plant and soil preparation

Lupins (*Lupinus albus* L. cv Feodora) were grown in aluminum containers (25 cm wide, 30 cm high and 1 cm thick) filled with sandy soil. The soil was collected from the artificial catchment of Chicken Creek located near Cottbus, Germany. The soil (sieved to a particle size smaller than 2 mm) consisted of 92% sand, 5% silt and 3% clay. The aluminum faces of the containers were detachable to allow filling of the soil. Three vertical sticks ($1 \times 30 \times 1$ cm) and three horizontal ones ($1 \times 25 \times 1$ cm) made of plastic were placed inside the containers, dividing the internal space of the containers into 16 compartments (four rows × four columns). The sandy soil was poured into each compartment through a 2 mm sieve to achieve a homogeneous soil deposition and to reduce soil layering while the containers were laid horizontally. The soil's DW was *c.* 1 kg in each container. The soil was wetted and the sticks were removed from the containers. The space between the compartments was filled with coarse sand (grain diameter 1.2–1.7 mm). The layers of coarse sand acted as capillary barriers to hydraulically disconnect the adjacent compartments without hindering root penetration. We refer to these layers as capillary barriers. The detachable faces of the containers were then closed, and the samples were gently turned vertically. This procedure resulted in an average bulk density of 1.4 g $cm^{-3}$. The detachable face of the containers had holes of 1 mm diameter at intervals of 3 cm. A fine-needle syringe was used for injecting $D_2O$ through the holes into the soil. The top of the samples was covered with a 1 cm layer of quartz gravel with a grain size of 3 mm to minimize evaporation.

Lupin seeds were germinated on moist filter paper in the dark for 24 h. The seedlings were then planted in the containers at 1 cm depth. The plants were grown for 18–21 d with a photoperiod of 14 h, light intensity of 300 µmol $m^2$ $s^{-1}$, day : night temperature of 24 : 19°C, and relative humidity of 60%. Plants were irrigated every third day by slowly immersing the samples in a nutrient solution until the water table reached the bottom of the upper compartments. The bottom of containers had holes to allow infiltration from underneath. The samples were then slowly lifted, allowing each compartment to drain freely. This resulted in an average water content of 0.20 $cm^3$ $cm^{-3}$ in each compartment. The nutrient solution was composed of: $K_2SO_4$, 3.5 mM; KCl, 1 mM; $KH_2PO_4$, 1 mM; $Ca(NO_3)_2$, 1 mM; $MgSO_4$, 5 mM; $H_3BO_3$, 100 µM; $MnSO_4$, 5 µM; $ZnSO_4$, 5 µM; $CuSO_4$, 2 µM; $(NH_4)Mo_7O_{24}$, 0.1 µM; and Fe-EDTA, 200 µM. The plants were 18–21 d old when the neutron radiography experiment started. Transpiration rates were calculated by weighing samples at intervals of 6 h during the day and night. The average daytime transpiration of 18- to 21-d-old plants was $1.23 \pm 0.18$ g $h^{-1}$ ($n = 10$) and it was negligible at night. At this stage, the plants had six leaves with a total leaf area of *c.* $63 \pm 5$ $cm^2$ ($n = 3$). After the measurement, we opened the containers and washed the roots. We did not observe any evidence of arbuscular mycorrhizas or rhizobial nodules.

### Neutron radiography

Neutron radiography is an imaging technique that, owing its high sensitivity to hydrous materials, has been widely used to image water and root distribution in soil (Tumlinson *et al.*, 2007; Moradi *et al.*, 2008; Oswald *et al.*, 2008; Carminati *et al.*, 2010). Neutron radiography consists of guiding a neutron beam across the sample. The transmitted beam carries the information about sample composition and thickness. The attenuation of the neutron beam through a sample is described by the Beer–Lambert law:

$$\frac{I}{I_0} = \exp^{-\sum_{i=1}^{i=n}(\mu_i d_i)}, \qquad \text{Eqn 1}$$

where $I$ is the intensity of the attenuated neutron beam (number of neutrons $m^{-2}$ $s^{-1}$), $I_0$ is the intensity of the incident neutron beam (number of neutrons $m^{-2}$ $s^{-1}$), $d_i$ (m) is the thickness of the $i$-material composing the sample, and $\mu_i$ ($m^{-1}$) is the macroscopic neutron attenuation coefficient, which describes the probability of neutron interactions with the materials per unit of thickness.

Our experiments were carried out at the ICON beam-line of the Paul Scherrer Institute (PSI), Switzerland. We used a charge-coupled device (CCD) camera detector with an array of $1260 \times 1260$ pixels, resulting in a field of view of $15.75 \times 15.75$ cm and an effective spatial resolution of 0.125 mm. Four radiographs with marginal overlaps were needed to scan a whole sample. For the measurements during the daytime, a lamp that was identical to those in the growth chamber was installed in the imaging station above the plants. Plants were kept in the imaging station for 1 h before starting the measurement. The measurements lasted *c.* 2 h. The transpiration rate was measured from the

weight of samples before and after neutron radiography. During daytime measurements, the average transpiration was $1.43 \pm 0.25\ g\ h^{-1}$ ($n = 4$).

## Deuterated water

Deuterated water was used as a contrast agent to trace the flow of water into the roots. In contrast to normal water, $D_2O$ has a much lower neutron attenuation coefficient, which makes it easily distinguishable in neutron radiographs. Because of its similarity to water, $D_2O$ has long been used to study water flow in plants (Ordin & Kramer, 1956; Matsushima *et al.*, 2008; Da-Ines *et al.*, 2010). We injected 3–4 ml of $D_2O$ (purity of 99.97%) locally in selected soil compartments using a syringe. The spatiotemporal distribution of $D_2O$ in soil and its transport into and along roots were monitored by time-series neutron radiography at time intervals of 10 s for a period of 2 h. The measurements were performed day and night at different locations for 10 samples.

## Image processing

Neutron radiographs were referenced to flat field (radiography without sample) and dark current (signal recorded by the camera when there was no beam). The neutron attenuations of aluminum and dry soil were determined by the neutron radiographs of a slab filled with dry soil. After subtraction of the contribution of aluminum and dry soil, the remaining values gave the water content in the sample. Owing to their high water content, the roots could be clearly distinguished from the soil. Roots were segmented from the soil using the roottracker two-dimensional (2D) algorithm developed by Anders Kaestner (Menon *et al.*, 2007). Root segmentation was performed on the radiographs obtained before the injection of $D_2O$. The segmented roots were skeletonized and their length and diameter were calculated using the Euclidean distance. In 2D radiographs, the signal in the pixels containing the roots was composed of attenuation coefficients of the roots and of the soil in front of and behind the roots in the beam direction (across soil thickness). The actual contributions of $H_2O$ and $D_2O$ in the roots were calculated assuming that the amounts of $H_2O$ and $D_2O$ in the soil in front of and behind the roots were equal to those of the soil at the sides of the roots (i.e. it we assumed a radial symmetry around the roots). We calculate the volumetric concentration of $D_2O$ in roots ($C_r$) and soil ($C_0$) as the thickness of $D_2O$ divided by the total liquid thickness in roots and soil, respectively. $C_r$ and $C_0$ were averaged along the segment of roots immersed in $D_2O$.

The volume of $D_2O$ transported beyond the capillary barrier was calculated by subtracting the radiographs at time $t$ from the radiograph before $D_2O$ injection. This image processing is described in details in the Supporting Information, Method S1, and in Zarebanadkouki *et al.* (2012).

## Model of $D_2O$ transport in roots

To quantify the radial flux of water into roots, Zarebanadkouki *et al.* (2012) introduced a simple model of $D_2O$ transport into and along roots. The transport of $D_2O$ into roots was described by a diffusion–convection model, where the transport rate of $D_2O$ into the roots depended on the convective transport (net root water uptake) and the diffusion of $D_2O$ (Fig. 1). Zarebanadkouki *et al.* (2012) assumed that the entire root segment, including the root tip, was immersed in $D_2O$ and the radial flow of water across the cortex was primarily apoplastic. In the present paper, the model is extended to the case when a portion of the root is immersed in $D_2O$, while the rest is immersed in normal water. Additionally, the description of the water flow across the cortex has been generalized to allow a variable importance of the apoplast and cell-to-cell pathways. The model is explained in the following sections. The derivation of the equations is given in Method S2.

The model is based on the observation that the increase of $D_2O$ was well fitted to the sum of two exponential curves.

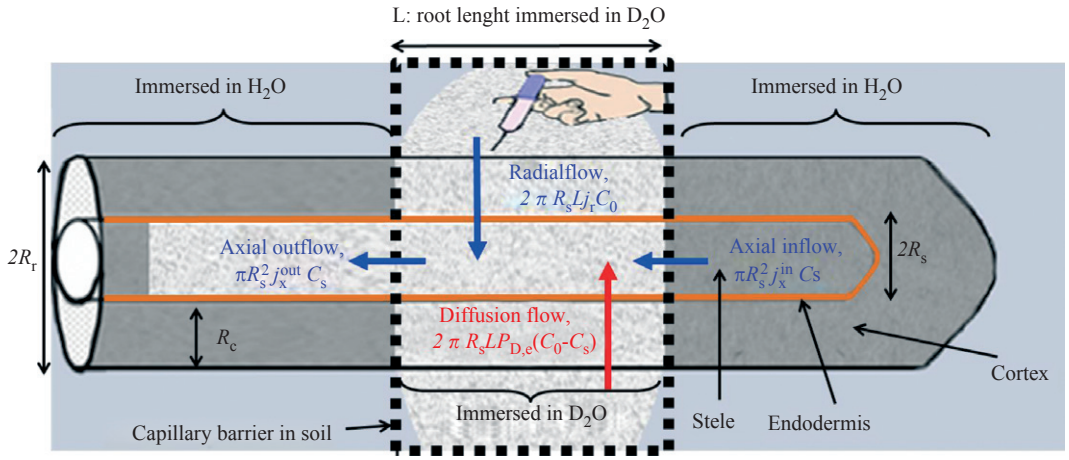


**Fig. 1** Illustration of deuterated water ($D_2O$) transport into a root that is partially immersed in $D_2O$. The radial transport of $D_2O$ into the root is driven by the concentration gradients between the soil and roots (diffusion, red arrows) and by convection following the transpiration stream (blue arrows). As $D_2O$ reaches the xylem, it mixes with the incoming water flow and flows axially along the root. The capillary barriers were used to limit $D_2O$ diffusion in soil. $C_s$, $C_0$, concentration of $D_2O$ in roots and soil, respectively; $R_r$, $R_s$, root and stele radii, respectively; $r_c$, radius of the cortical cell; $j_x^{in}$, axial flux of water into the root segment immersed in $D_2O$.

Statistical justification of the use of two exponential equations instead of a single exponential is given in Fig. S1. The two exponential rates were explained by the different dynamics of $D_2O$ transport into cortex and stele. The dynamics of $D_2O$ transport into cortex and stele depend not only on the diffusional permeability of the two compartments separated by the endodermis, but also on the axial flow along the roots. Imagine that a root segment is immersed in $D_2O$, while its proximal and distal segments are immersed in normal water. As normal water flows into the distal segment, $D_2O$ and normal water will mix according to the relative magnitudes of the radial and axial flow. The final concentration in the xylem of the segment immersed into $D_2O$ will converge to a lower value than the $D_2O$ concentration in soil and the rate of increase will be affected by the axial flow of the apical segment. Instead, the concentration in the cortex will converge to that of the soil, as the axial flow into the cortex is typically neglected. For this reason, the $D_2O$ dynamics in the stele and cortex are treated separately.

The average $D_2O$ concentration in the root, $C_r$, is calculated as the sum of the $D_2O$ concentration in the cortex, $C_c$, and the stele, $C_s$

$$C_r = \frac{(R_r - R_s)C_c + R_s C_s}{R_r}, \qquad \text{Eqn 2}$$

where $R_r$ and $R_s$ are the root and the stele radii, respectively.

We first consider the night-time experiments, when convection is assumed to be negligible. As mentioned earlier, our observations showed that the concentration of $D_2O$ in roots could be described by a double exponential model. The night-time increase of $C_{D_2O}$ in roots is described as

$$C_r = \frac{R_r - R_s}{R_r} C_0(1 - \exp^{-k_c^n t}) + \frac{R_s}{R_r} C_0(1 - \exp^{-k_s^n t}) \qquad \text{Eqn 3}$$

where $C_0$ is the $D_2O$ concentration in soil, and $k_c^n$ and $k_s^n$ are the rate constants of $D_2O$ concentration increase in the root cortex and the root stele, respectively, at night. Under the following assumptions, Eqn 3 can be demonstrated and the two rate constants have a physical meaning: the reflection coefficient of $D_2O$ across root membranes is approximated as zero, as measured by Henzler & Steudle (1995); $D_2O$ rapidly diffuses through the apoplast of the root cortex; and the endodermis is the main resistance to transport of $D_2O$ from the inner part of the cortex to the xylem vessels, with a consequent uniform $D_2O$ concentration inside the root stele. Note that the second assumption does not necessarily mean that there is significant $D_2O$ transport ($m^3\ s^{-1}$) across the apoplast. Under these assumptions, the parameters in Eqn 3 are

$$K_c^n = \frac{2P_{D,c}}{r_c}$$
$$K_s^n = \frac{2P_{D,e}}{R_s}, \qquad \text{Eqn 4}$$

where $P_{D,c}$ ($m\ s^{-1}$) is the diffusional permeability of the cortical cells, $r_c$ is the radius of the cortical cells, and $P_{D,e}$ ($m\ s^{-1}$) is the diffusional permeability of the endodermis. The diffusional permeability is defined as the diffusion coefficient of $D_2O$ across the membrane divided by the thickness of the membrane. In circumstances when the assumptions are not valid, Eqn 3 has to be considered as an empirical equation and the rate constants as effective diffusional parameters of cortex and stele.

During the daytime, transpiration results in a convective flow of water from soil to roots. Convective transport of $D_2O$ across the root (radial flow) and along the root (axial flow) need to be included in the model. The increase of $D_2O$ concentration in the roots during the day is described as

$$C_r = \frac{R_r - R_s}{R_r} C_0(1 - \exp^{-k_c^d t}) + \frac{R_s}{R_r}\beta C_0(1 - \exp^{-k_s^d t}), \qquad \text{Eqn 5}$$

where $k_c^d$ and $K_s^d$ are rate constants of the root cortex and the root stele during the daytime, respectively, and $\beta$ is a coefficient that describes the fact that when a root is only partly immersed in $D_2O$ its concentration does not converge to $C_0$ ($\beta \leq 1$) Under the assumptions, Eqn 5 can be explicitly derived and its parameters have the following physical meaning

$$K_c^d = \frac{2P_{D,c} + \lambda\frac{j_r}{2}}{r_c}$$
$$K_s^d = \frac{2P_{D,e}}{R_s} + \frac{j_x^{out}}{L}, \qquad \text{Eqn 6}$$
$$\beta = \frac{\frac{2P_{D,e}+2j_r}{R_s}}{\frac{2P_{D,e}}{R_s} + \frac{j_x^{out}}{L}}$$

where $j_r$ ($m\ s^{-1}$) is the radial flux of water into the root endodermis, $j_x^{out}$ ($m\ s^{-1}$) is the axial flux of water through the root stele from the root segment immersed in $D_2O$, $L$ is the length of the root segment immersed in $D_2O$, and $\lambda$ is a coefficient varying between zero and unity and describing the relative importance of the apoplastic and cell-to-cell flow across the cortex. If the flow through the cortex is purely apoplectic, $\lambda = 0$ and the model corresponds to that of Zarebanadkouki *et al.* (2012). If the flow though the cortex is purely cell to cell, $\lambda = 1$.

If the root segment including the root tip is entirely immersed in $D_2O$, the outflow of liquid from the root segment is equal to the radial flow into the segment ($\pi R_s^2 j_x^{out} = 2\pi R_s L j_r$). From Eqn 6 it follows that $\beta = 1$ and $k_s^d = 2(P_{D,e} + j_r)/R_s$. This case corresponds to the model of Zarebanadkouki *et al.* (2012). For the roots that are partly immersed in $D_2O$, the outflow of liquid from the root segment is equal to the radial convective flow into the segment plus the axial inflow of liquid into the root segment ($\pi R_s^2 j_x^{out} = 2\pi R_s L j_r + \pi R_s^2 j_x^{in}$. In this case, $\beta < 1$.

Eqns 3 and 5 were fitted to the data of the $D_2O$ concentration increase in the roots during the day and night that were obtained from neutron radiographs. From the night-time measurements, we calculated the diffusional permeabilities, $P_{D,c}$ and $P_{D,e}$. To calculate the net transport of $D_2O$ into the roots, we assumed that the diffusional permeability coefficients were identical during the day and night. The validity of this assumption is discussed later in the paper.

### Quantification of axial flux along the root

The axial fluxes, $j_x^{out}$, were directly calculated from the volume of $D_2O$ that passed the capillary barrier, $V_{D_2O}$ ($m^3$). $V_{D_2O}$ is related to the axial flow according to

$$\frac{dV_{D_2O}}{dt} = \pi R_s^2 j_x^{out} C_{s,b}(t), \quad \text{Eqn 7}$$

where $C_{s,b}$ is the $D_2O$ concentration in the root stele at the capillary barrier. $V_{D_2O}$ was quantified from the time-series neutron images. Note that the values obtained from Eqn 7 are independent of our modeling approach.

## Results

We measured the transport of $D_2O$ into the roots of 10 plants. $D_2O$ was injected into selected compartments of each sample during the day and night. To illustrate the results, we show the radiographs of one sample in which $D_2O$ was injected during the daytime into two compartments (Fig. 2). Fig. 2(a) shows radiography of the sample before the injection of 4 ml of $D_2O$ into each compartment. The image was obtained by overlapping four radiographs taken at different locations. A close-up of the regions where $D_2O$ was injected is shown in Fig. 2(b). In Fig. 2(a,b) the gray values are proportional to the water content: the darker the image, the higher the soil water content. Before $D_2O$ injection, the average soil water content in all compartments of the 10 samples was between 0.08 and 0.15 $cm^3\ cm^{-3}$, which in our soil corresponds to soil matric potentials of −70 and −20 hPa, respectively (Carminati *et al.*, 2010). After injection of $D_2O$, the water content increased from 0.08–0.15 to 0.18–0.25 $cm^3\ cm^{-3}$. The corresponding change in pressure is expected to be *c.* 50 hPa, which is small compared with the difference in water potential between soil and roots.

The sharp contrast between roots and the surrounding soil, resulting from the higher volumetric water content in roots, allowed us to segment roots from soil. The average root length of the 10 plants was 470 ± 36 cm ($n = 10$). The highlighted rectangles in Fig. 2(a) show the compartments where $D_2O$ was injected. The roots that were selected for the analysis of $D_2O$ transport are marked as roots 1–7 (Fig. 2b). Root 1, 2 and 4 were 12–14 cm long, and roots 3 and 7 were 8–10 cm long.

Fig. 2(c–e) shows the difference between the actual radiographs at time $t$ and the radiograph before $D_2O$ injection ($t = 0$). Brighter gray values indicate reduced neutron attenuation as a result of increased $D_2O : H_2O$ ratio. Conversely, the dark areas show accumulation of $H_2O$ after $D_2O$ injection. Fig. 2(c–e) shows that $D_2O$ quickly redistributed in the soil as a result of the rapid dissipation of pressure (bulk flow of $H_2O + D_2O$). The

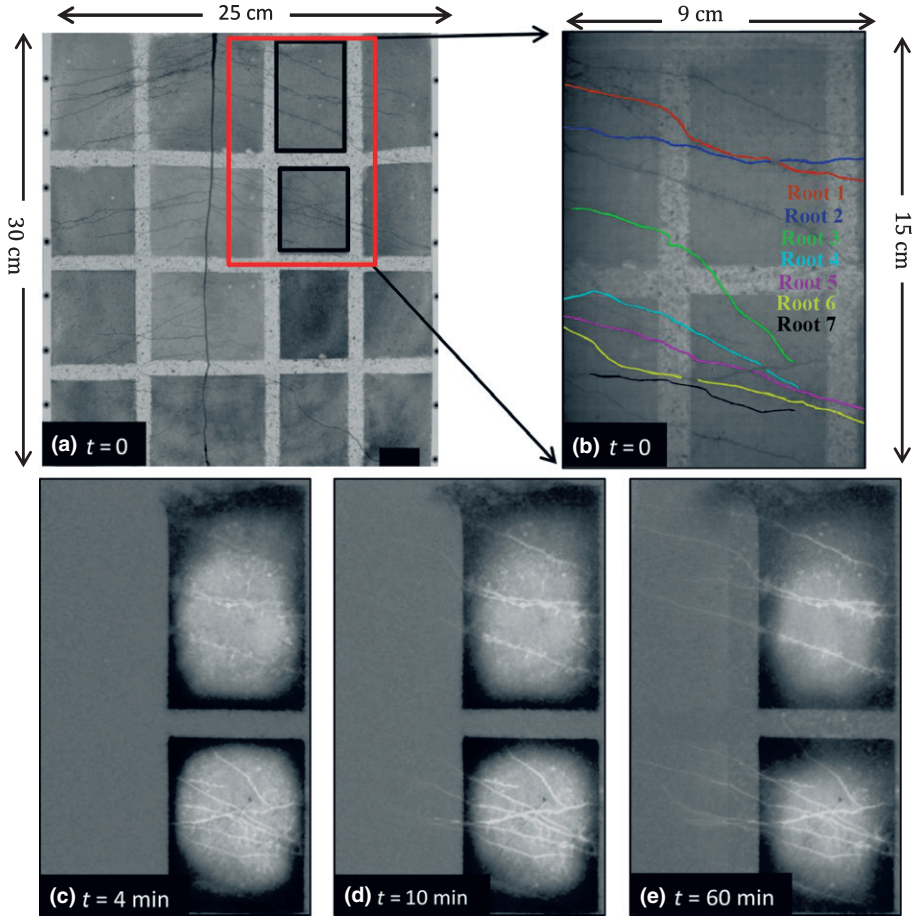


**Fig. 2** Neutron radiographs of one sample before (a, b) and after injection of 4 ml deuterated water ($D_2O$) (c–e) during the day. (a) Lupin (*Lupinus albus*) roots and soil water distribution. This image was obtained from stitching together four radiographs with an original field of view of 15.75 × 15.75 cm. The marked rectangles show the two compartments in which we injected $D_2O$ and monitored its transport into roots and soil. (b) Close-up of the original field of view showing the roots selected for the flow analysis. In panels (a) and (b), the darker the image, the wetter the soil. (c–e) The difference between the actual radiographs at time $t$ and the radiograph before $D_2O$ injection ($t = 0$). Here, brighter colors indicate lower neutron attenuation and higher $D_2O : H_2O$ ratio.

diffusive mixing of $D_2O$ and $H_2O$ appeared to be relatively slow. After injection, the roots turned bright, which indicated that $D_2O$ had entered them. As $D_2O$ entered the roots, it started to move along the root beyond the capillary barrier (Video S1). During the night-time, by contrast, $D_2O$ entered the roots more slowly and there was no $D_2O$ transport beyond the capillary barrier (Video S2).

Fig. 3(a) shows the transport of $D_2O$ into the taproot and laterals in the upper root zone (2–9 cm below the soil surface) at night. We injected 7 ml $D_2O$ into the middle compartment of the sample. The taproot turned bright more slowly than the lateral roots, indicating that the radial diffusive flow of $D_2O$ into the taproot was significantly slower than that into the lateral roots. Fig. 3(b) shows the increase of $D_2O$ concentration in the taproot (averaged in the segments at a distance of 24–25 cm from the root tip) and in the lateral roots (averaged in the segments at a distance of 10–12 cm from the root tip). These data are averaged for three roots and demonstrate that the taproot was less permeable than the lateral roots. For this reason, we expect that the role of the taproot in the absorption of water should be small and we focused our analysis on lateral roots.

For the quantification of $D_2O$ transport into roots, we selected the roots with minimum second-order laterals and cluster roots. We averaged the concentration of $D_2O$ in the centermost pixel of

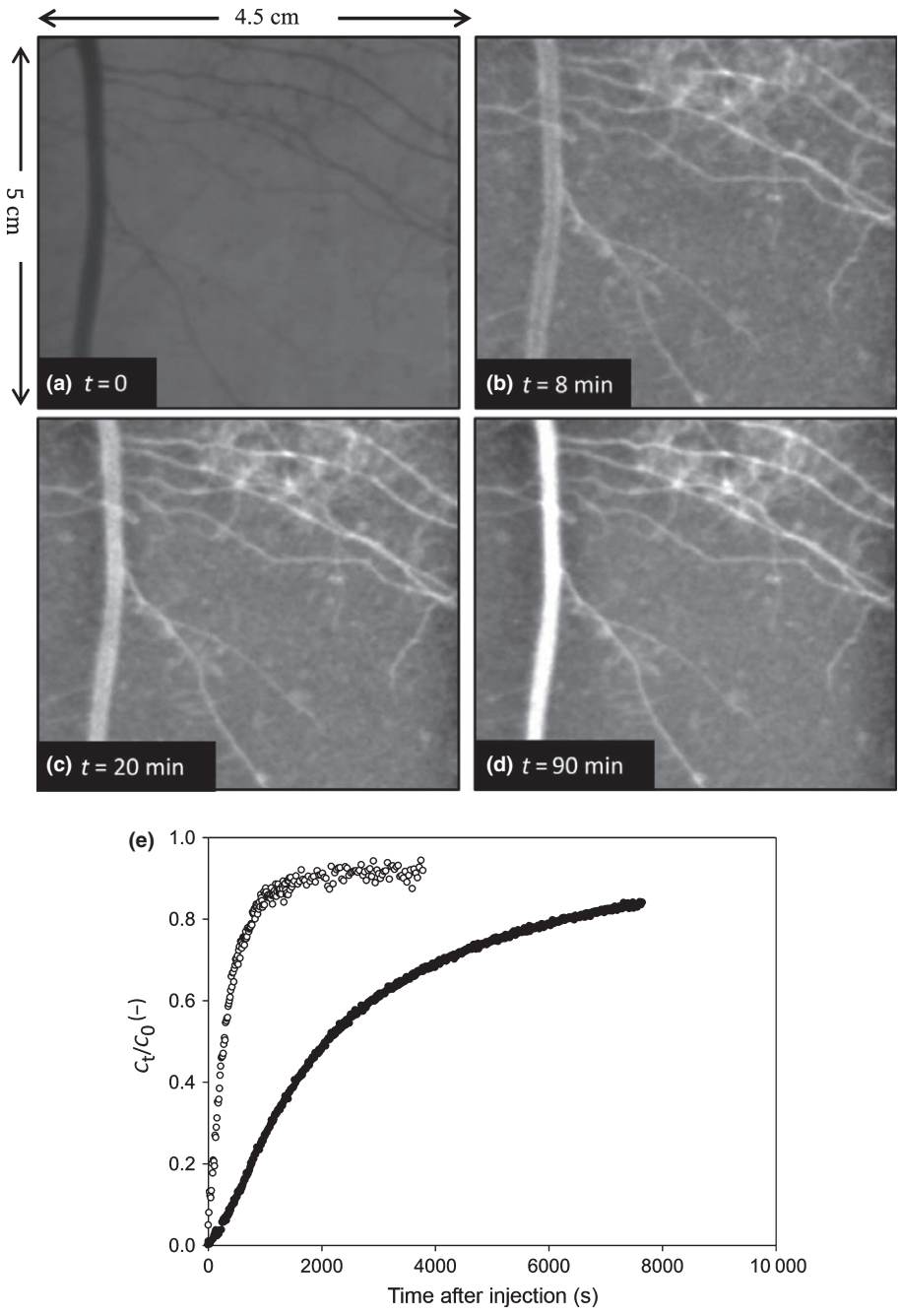


**Fig. 3** Neutron radiographs of one sample before deuterated water ($D_2O$) injection (a) and after injection (b–d) at night. (b–d) The difference between the actual radiograph at various times and that before injection (at $t = 0$). (a–d) Radial transport of $D_2O$ into the proximal parts of the Lupin (*Lupinus albus*) taproot (3–8 cm depth) and the lateral roots. Brighter colors in (b–d) indicate a higher $D_2O$ : $H_2O$ ratio. (e) The average concentration of $D_2O$ in the taproot (●, 24–25 cm) and in the laterals (○, 10–12 cm). The data are averaged for three plants. These results show that the taproot of lupins is less permeable than the laterals.

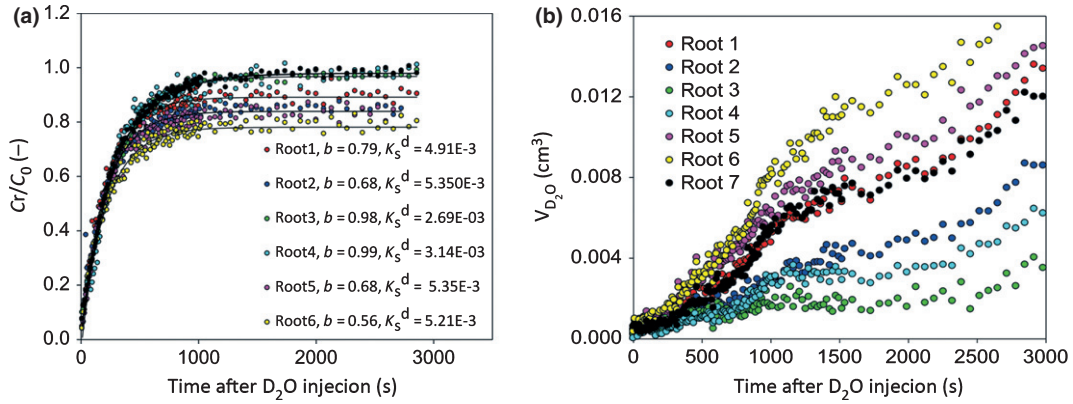


**Fig. 4** Increase of deuterated water ($D_2O$) concentration inside Lupin (*Lupinus albus*) roots (a), and volume of $D_2O$ passing beyond the barrier (b). The lines refer to the roots marked in Fig. 2. The experiment was performed during the daytime. The concentrations were averaged along the segment of roots that were immersed in $D_2O$. $D_2O$ concentrations in roots were fitted using Eqn 5. The fitted parameters are presented in the legend for each root.

**Table 1** Diffusional permeability of cortical cells, $P_{D,c}$ ($m\,s^{-1}$), and endodermis, $P_{D,e}$ ($m\,s^{-1}$), along lateral roots

| Distance from tip (cm) | Diffusional permeability of cortical cells, $P_{D,c}$ ($m\,s^{-1}$) | Diffusional permeability of endodermis, $P_{D,e}$ ($m\,s^{-1}$) |
|---|---|---|
| 2–3 | $5.0 \pm 0.4 \times 10^{-8}$ | $1.4 \pm 0.2 \times 10^{-7}$ |
| 7–8 | $4.6 \pm 0.2 \times 10^{-8}$ | $1.0 \pm 0.1 \times 10^{-7}$ |
| 10–12 | $4.6 \pm 0.3 \times 10^{-8}$ | $5.6 \pm 0.3 \times 10^{-8}$ |

Diffusional permeabilities were measured at various distances from the root tip using the data of $D_2O$ transport into the roots at night, when transpiration was nearly zero. The values are the average of six roots.

the root segment immersed in $D_2O$. At night, $D_2O$ concentration in the roots increased to a maximum value identical to that of the soil at the root surface (data not shown). During the day, $D_2O$ concentration in the roots rapidly increased to a maximum that varied among roots. Fig. 4(a) shows the average $D_2O$ concentration in the roots highlighted in Fig. 2.

We calculated the diffusional permeability of the cortical cells, $P_{D,c}$, and the endodermis, $P_{D,e}$, by fitting the night-time measurements with Eqn 3. The radii of the root stele ($R_s = 150 \pm 0.1$ µm, $n = 5$) and the cortical cell ($r_c = 23 \pm 0.05$ µm, $n = 20$) were obtained through microscopic observation of the root cross-sections (Zarebanadkouki *et al.*, 2012). $P_{D,c}$ and $P_{D,e}$ at three locations along the laterals are reported in Table 1. The diffusional permeability of cortical cells showed no variation along the roots and had an average value of $4.8 \pm 0.3 \times 10^{-8}\,m\,s^{-1}$. By contrast, the diffusional permeability of the endodermis decreased from $1.4 \pm 0.2 \times 0.210^{-7}\,m\,s^{-1}$ in the most distal parts of the roots (2–3 cm from the root tip) to $5.6 \pm 0.3 \times 10^{-8}\,m\,s^{-1}$ in the most proximal parts (10–12 cm from the root tip).

By fitting the increase of $D_2O$ concentration in roots using Eqn 5, we obtained the radial flux, $j_r$, the axial flux, $j_x^{out}$, and the parameter $\lambda$. To summarize the results, we grouped the roots of 10 plants into an upper zone (roots at 2–9 cm below the soil surface) and a lower zone (18–27 cm below the soil surface). Additionally we grouped the roots according to their length into: long roots, of length 12–14 cm; medium roots, of length 8–10 cm; and short roots, of length 3–4 cm. These groups yield a picture of the distribution of root water uptake along the root system, as presented in Fig. 5.

To quantify the results, we first started with the middle segments (distance of 6–9 cm from the root tip) of long roots (12–14 cm long). For these root segments, the axial fluxes, $j_x^{out}$, were calculated from Eqn 7 using the volume of $D_2O$ passing beyond the capillary barrier. Fig. 4(b) shows the volume of $D_2O$ passing the capillary barrier in different roots of the sample presented in Fig. 2. A few seconds after $D_2O$ injection, we observed the transport of $D_2O$ beyond the capillary barrier. The volume of $D_2O$ passing the capillary barrier increased gradually in the beginning, because the $D_2O$ concentration in the root xylem was increasing. After *c.* 200 s, when the $D_2O$ concentration in the root at the capillary barrier reached a constant value, $V_{D_2O}$ started to increase linearly with time. The linear behavior was observed until 1200 s, when the $D_2O$ front reached the taproot and exited the field of view. The values of $j_x^{out}$ were calculated according to Eqn 7 using the linear phase of the curves. The remaining parameters $j_r$ and $\lambda$ were derived from fitting the data from daytime measurement using Eqn 5. The best fit was obtained with $\lambda = 0.14 \pm 0.1$ ($n = 10$). The results of curve fittings for the sample presented in Fig. 2 are given in Fig. 4(a). For the remaining roots we set $\lambda = 0.14$ and we calculated $j_r$ and $j_x^{out}$. This fitting procedure was chosen because the independent estimation of $j_x^{out}$ from Eqn 7 was not possible for the root segments near the taproot.

The results of the radial flux calculations at different locations of 10 plants are summarized in Fig. 5. The calculated radial fluxes showed significant variation along the roots. The radial fluxes into lateral roots were higher in the upper zone than in the lower zone. The radial fluxes into the most proximal segments of long and short roots were *c.* three to four times higher in the upper zone than in the lower zone. The radial fluxes in the more distal parts were six times higher in the upper than in the lower zone.

Looking at individual laterals, the highest radial fluxes were seen in the most proximal segments, and they declined towards the distal segments (near the root tip). For the long roots in the upper zone, the radial flux into the most proximal segments

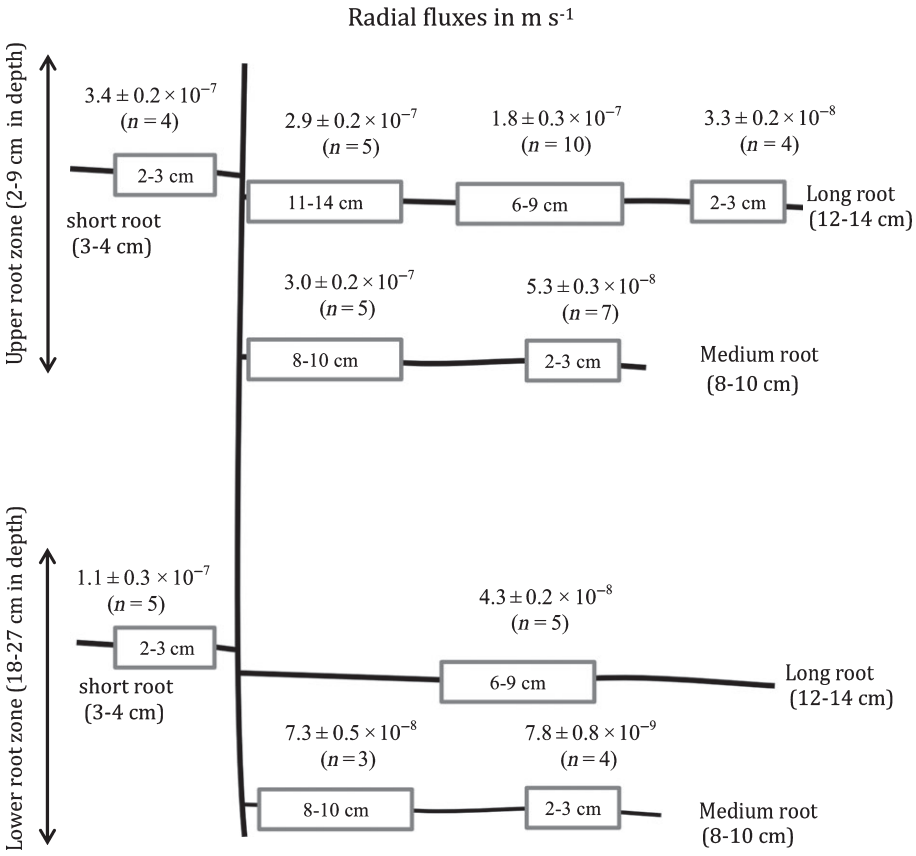


**Fig. 5** Scheme of the root system showing the distribution of the radial fluxes, $j_r$ (m s$^{-1}$), calculated with Eqn 5. Roots are grouped into upper zone and lower root zone according to their depth. Roots were additionally grouped into categories of long, medium and short roots. The numbers inside the boxes indicate the distance from the root tip. The value of radial flux for each position is averaged for *n* replications and is given above the boxes in m s$^{-1}$. The results are averaged among 10 samples.

(11–14 cm from the root tip) was twice as high as into the middle segments (6–9 cm from the root tip), and nine times higher than that into the distal segments (2–3 cm from the root tip). For the medium roots in the upper zone, the radial flux into the most proximal segments (8–10 cm from the root tip) was six times higher than into the distal segments (2–3 cm from the root tip). For the medium roots in the lower region, the flux into the proximal segments was nine times higher than into the distal segments.

The radial flux into the root endodermis predicted by the model agreed well with independent measurements of average root water uptake. Taking the average total root length (470 cm), the average water consumption (1.43 g h$^{-1}$) and the radius of the endodermis (150 μm), we obtained an average radial flux into the endodermis equal to $8.9 \times 10^{-8}$ m s$^{-1}$, which agrees well with the values predicted by the model (Fig. 5).

The axial fluxes at different locations of the long and medium lateral roots calculated from the model (Eqn 5) and those obtained directly from Eqn 7 are shown in Fig. 6. The highest axial fluxes were found in the more proximal parts of the roots: $2.9 \pm 0.2 \times 10^{-4}$ m s$^{-1}$ for long roots, and $2.1 \pm 0.2 \times 10^{-4}$ m s$^{-1}$ for medium roots.

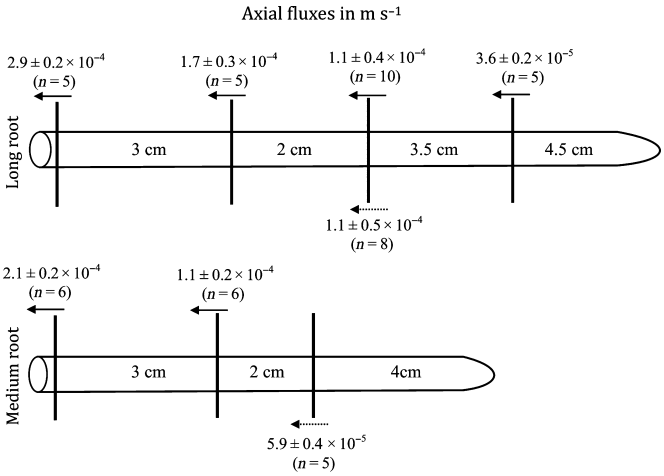


**Fig. 6** Axial fluxes, $j_x^{out}$ (m s$^{-1}$), in long and medium roots calculated from the model (Eqn 5, solid arrows above roots) and obtained directly from radiographs (Eqn 7, dashed thin arrows below roots). The numbers inside the roots indicate the distance between each root segment. Note that the axial fluxes are calculated for the cross-section of the root stele.

## Discussion

The transport of $D_2O$ into the roots showed a double exponential growth over time. This was explained by a different rate of $D_2O$ transport into the cortical cells and the root stele; and the dilution of $D_2O$ concentration in the root stele as a result of the inflow of normal water into the xylem during transpiration (when distal parts of roots were not immersed in $D_2O$). We developed a simple diffusion–convection model to describe the local transport of $D_2O$ into roots. The radial transport through the cortex included both an apoplastic and a cell-to-cell pathway.

The relative importance of the two pathways varied with the parameter $\lambda$. The best fit was obtained with $\lambda = 0.14$, which suggests a dominant apoplastic flow through the cortex. Note that the model says nothing about the relative importance of the two pathways across the whole root: that is, it may be that the apoplast at the endodermis is completely interrupted and that the overall root conductivity is controlled by the cell-to-cell pathway. By fitting the neutron radiograph data, the model calculated the diffusional permeabilities of the cortical cells and the endodermis and the radial and axial fluxes of water in different root segments. The results demonstrated significant variations in water uptake rate along the root system. The radial fluxes were higher in the upper zone than in the lower zone. In each root, the radial fluxes were higher in the more proximal segments and decreased towards the distal segments.

Lower water uptake in the distal segments of lateral roots could be explained by lower radial conductivity of the distal segments and/or significant dissipation of the water potential along the root system (driving force). The night-time experiments showed that $D_2O$ entered the distal segments more quickly than the proximal ones. This indicates that the radial permeability of roots was higher in the distal segments than in the proximal ones. A more likely explanation of the lower water uptake in the distal segments is that there was a significant dissipation of water potential along the xylem of lateral roots. Owing to the porous nature of roots, the relative importance of radial and axial conductivity determines the distribution of water potential and water uptake along the root (Landsberg & Fowkes, 1978; Frensch *et al.*, 1996; Hsiao & Xu, 1995; Zwieniecki *et al.*, 2003). The high ratio of radial to axial conductivity results in a higher dissipation of water potential along roots and, consequently, in hydraulic 'isolation' of the distal segments. In the lateral roots, incomplete development of the xylem vessels towards distal segments would produce lower axial conductivity and may have further decreased the water uptake in the most apical parts (McCully & Canny, 1988; Huang & Nobel, 1993; McCully, 1995; Bramley *et al.*, 2009).

The decrease in water uptake with distance was smaller in the proximal than in the lateral segments. In lateral segments, water uptake decreased ninefold over a distance of 10 cm from the proximal segments to the distal ones (2–3 cm from the tips). By contrast, water uptake into the proximal segments of roots decreased three- to fourfold over a depth of 15 cm (Fig. 5). This indicates that the dissipation of water potential for the same unit of the root length along the taproot is less significant than along lateral roots. The low dissipation of water potential along the taproot is explained by the low ratio of radial to axial conductivity. Indeed, the microscopic observation of the root cross-sections revealed that xylem vessels were larger and more abundant in the taproot than in the lateral roots (data not shown). Additionally, night-time experiments showed that the radial transport of $D_2O$ into the taproot was significantly slower than into the lateral roots (Fig. 3). This indicates that, in comparison to lateral roots, the taproot is significantly more resistant to radial flow of water into roots. The function of the taproot is to collect water from laterals and transport it to the shoot. The combination of high axial conductivity and low radial conductivity is beneficial for collecting water from deep in the soil and for increasing the portion of roots involved in water uptake. The taprooted architecture seems optimal for plant survival in soils where water is mainly stored in the deep profiles.

Our observations of higher radial fluxes at the more proximal segments of roots are in agreement with modeling studies (Landsberg & Fowkes, 1978; Doussan *et al.*, 1998), experiments with excised roots (Frensch & Steudle, 1989; Zwieniecki *et al.*, 2003), and those with roots in soils (Doussan *et al.*, 2006). The location of root water uptake is expected to change with root maturation. A decrease of radial hydraulic conductivity and an increase of axial conductivity as a result of root maturation might move the location of water uptake to more distal zones. Sanderson (1983) measured the profile of water uptake along roots of barley grown in hydroponics culture using a potometer apparatus. He found that the peak of water uptake was at a distance of 4–5 cm from the tip. Varney & Canny (1993) measured water uptake of lateral and axile roots for aeroponically grown maize. They observed that the maximum uptake from the laterals occurred at 30–60 cm from the root tip of the main axes, and decreased towards the tip and the proximal parts. The axile roots were *c.* 100 cm long. Variations in root architecture, maturation of xylem vessels, changes of root permeability by root maturation, and different growth conditions account for the discrepancy in the proximal parts.

As already discussed, the ratio of axial to radial conductivities determines the profile of water uptake along a root. In order to maintain a large area of roots involved in water uptake, root elongation needs to be coupled with a decrease in radial conductivity and an increase in axial conductivity. In addition to irreversible modification of roots during maturation, the ratio of radial to axial resistance might be regulated by aquaporins and also by the resistance of the root–soil interface. Recent studies on water dynamics in the rhizosphere showed that when the soil dries, the rhizosphere becomes temporarily hydrophobic (Carminati *et al.*, 2010). Such a temporary hydrophobicity may help plants to isolate the roots from the top dry soil and favor the uptake from the deep wet soil (Carminati, 2012). A similar mechanism will happen when roots shrink and lose contact with the soil (Nobel & Cui, 1992; Nye, 1994; North & Nobel, 1997; Carminati *et al.*, 2012). Carminati *et al.* (2012) used X-ray computed tomography (CT) to monitor the formation of air-filled gaps between soil and roots of lupins. They found that gaps occurred mainly around the taproot. As we have shown that the taproot is not that important for water uptake, gaps seem not to represent a limitation for water uptake. Such rhizosphere dynamics and gap formation are reversible and their role in plant adaptation to drought needs further investigation.

Some assumptions of the model of $D_2O$ transport in soil and roots need to be further investigated, with consequent improvement of the model. We assumed that after $D_2O$ injection, $D_2O$ moved rapidly by diffusion and convection in the apoplast of the root cortex. With this assumption, our model can be explicitly derived and the parameters have a physical meaning. The diffusion time of $D_2O$ in the apoplast of the cortex is given by

$t = l^2/(2D)$, where $l$ is the diffusional length and $D$ is the diffusion coefficient of $D_2O$ in $H_2O$ through the apoplast of the cortex. The diffusional length is given by the thickness of the cortex, $l = 1.5 \times 10^{-4}$ m. The diffusion coefficient of $D_2O$ in pure water is $D = 2.27 \times 10^{-9}\ m^2\ s^{-1}$ (Longsworth, 1995). This value would give a diffusional time of $t = 5$ s, which is consistent with our hypothesis. However, the diffusion of $D_2O$ is slower in the apoplast than in pure water. Richter & Ehwald (1983) observed that diffusivity of sucrose (molecular weight of 342 g $mol^{-1}$) in the extracellular space of sugar beet was five to 10 times lower than in water. Aikman *et al.* (1980) reported a 10-fold decrease for $Rb^+$ diffusion. The diffusivity of charged and large molecules is expected to be reduced more significantly than that of a neutral and low-molecular-weight molecule like $D_2O$ (Aikman *et al.*, 1980; Richter & Ehwald, 1983; Fleischer & Ehwald, 1995; Fritz & Ehwald, 2011). A 10-fold reduction in $D$ therefore seems a safe assumption and would give a diffusional time of 50 s. This value is still smaller than the half time of the $D_2O$ concentration increase in roots during night that was *c.* 300 s (Zarebanadkouki *et al.*, 2012). A second assumption that needs further investigation is whether or not the diffusional permeability of cortical cells and the endodermis is constant during the day and night. It is known that aquaporin activity is a function of transpiration and therefore it would affect the diffusional permeabilities (Maurel *et al.*, 2008). Bramley *et al.* (2009) showed that the radial flow of water in lupin roots occurred primarily through the apoplast, with a negligible involvement of aquaporins, while in wheat the water flow mainly occurred via cell-to-cell pathways. Our assumption of constant diffusional permeability of the endodermis during the day and night may therefore be justified for lupin roots, but it should be improved before application to other plant species. Future improvements of the model should include the diffusion of $D_2O$ though the apoplast of the cortex, which is now assumed to be instantaneous, and a variable $P_d$ during the day and night. Further experiments with plant species that are known to have a dominant cell-to-cell pathway would be greatly beneficial to test the model.

## Acknowledgements

The doctoral position of M.Z. was funded by the IPSWaT scholarship program (under stipend IPS 11/Q04) from the German Federal Ministry of Education and Research (BMBF). We thank Anders Kaestner and Stefan Hartmann from the Paul Scherrer Institute, Switzerland, for their valuable technical support during the measurements using neutron radiography. We thank M.J. Canny for his comments and suggestions regarding a previous version of this manuscript.

## References

**Aikman DP, Harmer R, Rust TSO. 1980.** Electrical resistance and ion movement through excised discs of sugar beet root tissue. *Physiologia Plantarum* **48**: 395–402.

**Bramley H, Turner NC, Turner DW, Tyerman SD. 2009.** Roles of morphology, anatomy, and aquaporins in determining contrasting hydraulic behavior of roots. *Plant Physiology* **150**: 348–364.

**Carminati A. 2012.** A model of root water uptake coupled with rhizosphere dynamics. *Vadose Zone Journal* **11**: doi:10.2136/vzj2011.0106.

**Carminati A, Moradi AB, Vetterlein D, Vontobel P, Lehmann E, Weller U, Vogel H-J, Oswald SE. 2010.** Dynamics of soil water content in the rhizosphere. *Plant and Soil* **332**: 163–176.

**Carminati A, Vetterlein D, Koebernick N, Blaser S, Weller U, Vogel H-J. 2012.** Do roots mind the gap? *Plant and Soil.* doi: 10.1007/s11104-012-1496-9.

**Da-Ines O, Graf W, Franck KI, Albert A, Winkler JB, Scherb H, Stichler W, Schäffner AR. 2010.** Kinetic analyses of plant water relocation using deuterium as tracer–reduced water flux of Arabidopsis pip2 aquaporin knockout mutants. *Plant Biology* **12**: 129–139.

**Doussan C, Page L, Vercambre G. 1998.** Modelling of the hydraulic architecture of root systems: an integrated approach to water absorption – model description. *Annals of Botany* **81**: 213–223.

**Doussan C, Pierret A, Garrigues E, Pagès L. 2006.** Water uptake by plant roots: II modelling of water transfer in the soil root-system with explicit account of flow within the root system – comparison with experiments. *Plant and Soil* **283**: 99–117.

**Draye X, Kim Y, Lobet G, Javaux M. 2010.** Model-assisted integration of physiological and environmental constraints affecting the dynamic and spatial patterns of root water uptake from soils. *Journal of Experimental Botany* **61**: 2145–2155.

**Enstone DE, Peterson CA, Ma F. 2003.** Root endodermis and exodermis: structure, function, and responses to the environment. *Journal of Plant Growth Regulation* **21**: 335–351.

**Fleischer A, Ehwald R. 1995.** The free space of sugars in plant tissues6. *Journal of Experimental Botany* **46**: 647–654.

**Frensch J, Hsiao TC, Steudle E. 1996.** Water and solute transport along developing maize roots. *Planta* **198**: 348–355.

**Frensch J, Steudle E. 1989.** Axial and radial hydraulic resistance to roots of maize (*Zea mays* L.). *Plant Physiology* **91**: 719–726.

**Fritz M, Ehwald R. 2011.** Mannitol permeation and radial flow of water in maize roots. *New Phytologist* **189**: 210–217.

**Garrigues E, Doussan C, Pierret A. 2006.** Water uptake by plant roots: I formation and propagation of a water extraction front in mature root systems as evidenced by 2d light transmission imaging. *Plant and Soil* **283**: 83–98.

**Henzler T, Steudle E. 1995.** Reversible closing of water channels in Chara internodes provides evidence for a composite transport model of the plasma membrane. *Journal of Experimental Botany* **46**: 199–209.

**Hsiao TC, Xu LK. 2000.** Sensitivity of growth of roots versus leaves to water stress: biophysical analysis and relation to water transport. *Journal of Experimental Botany* **51**: 1595–1616.

**Huang B, Nobel PS. 1993.** Hydraulic conductivity and anatomy along lateral roots of cacti: changes with soil water status. *New Phytologist* **123**: 499–507.

**Javaux M, Schröder T, Vanderborght J, Vereecken H. 2008.** Use of a three-dimensional detailed modeling approach for predicting root water uptake. *Vadose Zone Journal* **7**: 1079–1088.

**Knipfer T, Fricke W. 2010.** Water uptake by seminal and adventitious roots in relation to whole-plant water flow in barley (*Hordeum vulgare* L.). *Journal of Experimental Botany* **62**: 717–733.

**Landsberg JJ, Fowkes ND. 1978.** Water movement through plant roots. *Annals of Botany* **42**: 493–508.

**Longsworth L. 1960.** The mutual diffusion of light and heavy water. *Journal of Physical Chemistry* **64**: 1914–1917.

**Matsushima U, Kardjilov N, Hilger A, Graf W, Herppich WB. 2008.** Application potential of cold neutron radiography in plant science research. *Journal of Applied Botany and Food Quality* **82**: 90–98.

**Maurel C, Verdoucq L, Luu D-T, Santoni V. 2008.** Plant aquaporins: membrane channels with multiple integrated functions. *Annual Review of Plant Biology* **59**: 595–624.

**McCully M. 1995.** How do real roots work?(Some new views of root structure). *Plant Physiology* **109**: 1–6.

**McCully ME, Canny MJ. 1988.** Pathways and processes of water and nutrient movement in roots. *Plant and Soil* **111**: 159–170.

**Menon M, Robinson B, Oswald SE, Kaestner A, Abbaspour KC, Lehmann E, Schulin R. 2007.** Visualization of root growth in heterogeneously contaminated soil using neutron radiography. *European Journal of Soil Science* **58**: 802–810.

**Moradi AB, Carminati A, Vetterlein D, Vontobel P, Lehmann E, Weller U, Hopmans JW, Vogel H-J, Oswald SE. 2011.** Three-dimensional visualization and quantification of water content in the rhizosphere. *New Phytologist* **192**: 653–663.

**Moradi AB, Conesa HM, Robinson B, Lehmann E, Kuehne G, Kaestner A, Oswald S, Schulin R. 2008.** Neutron radiography as a tool for revealing root development in soil: capabilities and limitations. *Plant and Soil* **318**: 243–255.

**Nobel PS, Cui M. 1992.** Hydraulic conductances of the soil, the root-soil air gap, and the root: changes for desert succulents in drying soil. *Journal of Experimental Botany* **43**: 319–326.

**North GB, Nobel PS. 1997.** Drought-induced changes in soil contact and hydraulic conductivity for roots of *Opuntia ficus-indica* with and without rhizosheaths. *Plant and Soil* **191**: 249–258.

**Nye PH. 1994.** The effect of root shrinkage on soil water inflow. *Philosophical Transactions of the Royal Society of London Series B* **345**: 395–402.

**Ordin L, Kramer PJ. 1956.** Permeability of *Vicia faba* root segments to water as measured by diffusion of deuterium hydroxide. *Plant Physiology* **31**: 468–471.

**Oswald SE, Menon M, Carminati A, Vontobel P, Lehmann E, Schulin R. 2008.** Quantitative imaging of infiltration, root growth, and root water uptake via neutron radiography. *Vadose Zone Journal* **7**: 1035–1047.

**Pierret A, Kirby M, Moran C. 2003.** Simultaneous X-ray imaging of plant root growth and water uptake in thin-slab systems. *Plant and Soil* **255**: 361–373.

**Pohlmeier A, Oros-Peusquens A, Javaux M, Menzel MI, Vanderborght J, Kaffanke J, Romanzetti S, Lindenmair J, Vereecken H, Shah NJ. 2008.** Changes in soil water content resulting from *Ricinus* root uptake monitored by magnetic resonance imaging. *Vadose Zone Journal* **7**: 1010–1017.

**Richter E, Ehwald R. 1983.** Apoplastic mobility of sucrose in storage parenchyma of sugar beet. *Physiologia Plantarum* **58**: 263–268.

**Sanderson J. 1983.** Water uptake by different regions of the barley root. Pathways of radial flow in relation to development of the endodermis. *Journal of Experimental Botany* **34**: 240–253.

**Steudle E, Peterson CA. 1998.** How does water get through roots? *Journal of Experimental Botany* **49**: 775–788.

**Tumlinson LG, Liu H, Silk WK, Hopmans JW. 2007.** Thermal neutron computed tomography of soil water and plant roots. *Soil Science Society of America Journal* **72**: 1234–1242.

**Varney GT, Canny MJ. 1993.** Rates of water uptake into the mature root system of maize plants. *New Phytologist* **123**: 775–786.

**Vercambre G, Doussan C, Pages L, Habib R, Pierret A. 2002.** Influence of xylem development on axial hydraulic conductance within *Prunus* root systems. *Trees* **16**: 479–487.

**Zarebanadkouki M, Kim YX, Moradi AB, Vogel H-J, Kaestner A, Carminati A. 2012.** Quantification and modeling of local root water uptake using neutron radiography and deuterated water. *Vadose Zone Journal* **11**: doi: 10.2136/vzj2011.0196.

**Zwieniecki MA, Thompson MV, Holbrook NM. 2003.** Understanding the hydraulics of porous pipes: tradeoffs between water uptake and root length utilization. *Journal of Plant Growth Regulation* **21**: 315–323.

## Supporting Information

Additional supporting information may be found in the online version of this article.

**Fig. S1** Measured $D_2O$ concentration inside the roots and the best-fit lines using a single and double exponential equation.

**Method S1.** Details of image processing.

**Method S2**. Derivation of the model of $D_2O$ transport into roots.

**Video S1** $D_2O$ injection during daytime.

**Video S2** $D_2O$ injection into two compartments during night-time.

Please note: Wiley-Blackwell are not responsible for the content or functionality of any supporting information supplied by the authors. Any queries (other than missing material) should be directed to the *New Phytologist* Central Office.